Enhanced initial proliferation and differentiation of MC3T3-E1 cells on HF/HNO_3 solution treated nanostructural titanium surface

Fuming He, MD, DDS,[a] Feng Zhang, PhD, DDS,[b] Guoli Yang, PhD, DDS,[c] Xiaoxiang Wang, PhD,[d] and Shifang Zhao, MD, DDS,[e] Hangzhou, China
ZHEJIANG UNIVERSITY

Objective. The aim of this study was to investigate the effects of nano- or submicro topography and fluoride ion on the biology of osteoblasts.
Study design. Pure Ti plates were sandblasted, etched with an HCl/H_2SO_4 solution (control surface) and then etched in a diluted HF/HNO_3 solution (test surface). MC3T3-E1 cells attached, spread, and proliferated on both surfaces.
Results. The alkaline phosphatase activity was evidently higher for the test surface than for control surface after 4 and 7 days of cell culture. Real-time PCR showed significant increases in type I collagen and osteocalcin gene expression in osteoblast growth on the test surface after 4 days of culture compared with the control surface.
Conclusion. With nanotopography and fluoride, hydrogen ions might improve MC3T3-E1 cell proliferation and differentiation during the early stages of cell culture. **(Oral Surg Oral Med Oral Pathol Oral Radiol Endod 2010;xx: xxx)**

The development of novel mechanical and chemical surface modification treatments to improve the osseointegration properties of dental implants is a topic of great interest.[1] Surface characteristics determine tissue reactions to an oral implant. The surface topography relates to the degree of surface roughness and the orientation of surface irregularities. Surface roughness has been the main focus of oral implants for more than a decade.[2] Surface sandblasting and acid etching (SLA) can increase the rate and amount of bone formation onto an implant surface.[3-5]

Financial support from the Key Scientific and Technological Project Fund of Zhejiang province (Grant No. 2008C13025-2, China) is gratefully acknowledged.
[a]Associate doctor, Department of Implantology, The Affiliated Stomatology Hospital, School of Medicine, Zhejiang University, Hangzhou, China.
[b]Attending doctor, Department of Oral and Maxillofacial Surgery, The Affiliated Stomatology Hospital, School of Medicine, Zhejiang University, Hangzhou, China.
[c]Attending doctor, Department of Implantology, The Affiliated Stomatology Hospital, School of Medicine, Zhejiang University, Hangzhou, China.
[d]Professor, Department of Materials Science and Engineering, Zhejiang University, Hangzhou, China.
[e]Professor, Department of Oral and Maxillofacial Surgery, The Affiliated Stomatology Hospital, School of Medicine, Zhejiang University, Hangzhou, China.
Received for publication Dec 17, 2009; returned for revision Mar 18, 2010; accepted for publication Mar 24, 2010.
1079-2104/$ - see front matter

doi:10.1016/j.tripleo.2010.03.044

Several cell culture studies,[6-9] preclinical animal investigations,[10-13] and clinical trials[14] have supported the observation that hydrofluoric acid treatment of TiO_2 grit-blasted titanium implants is associated with rapid bone accrual at the implant surface. It has been reported that fluoride ion treatment of TiO_2 grit-blasted titanium substrates enhances adherent osteoblastic differentiation and bone sialoprotein, and BMP-2 expression of human mesenchymal stem cells. It also significantly increases the bone-to-implant contact at TiO_2 grit-blasted commercially pure titanium implants in the rat tibia model.[7] Osteoblast growth on a moderately rough etched fluoride-modified titanium surface was compared with osteoblast growth on the same surface grit-blasted with titanium dioxide; the Cbfa1 (a key regulator for osteogenesis) expression on the fluoride-modified titanium surface was significantly higher at 1 week.[6] The results indicated that fluoride-modified surface topography, in synergy with surface roughness, may have a greater influence on the level of expression of Cbfa1 than the unmodified titanium surfaces studied. Fluoride-modification of dental titanium (Ti) implants has been showed to improve peri-implant bone growth and bone-to-implant contact and adhesion strength.[10-13] It is suggested that the fluoride-modified implant surface promotes osseointegration in the early phase of healing following implant installation.[12] Treatment with hydrofluoric acid can create discrete nanostructures on a TiO_2 grit-blasted surface.[15] Nanoscale modification of titanium endosseous implant surfaces may alter cellular and tissue responses that may benefit osseointegration and

dental implant therapy.[16] The characteristic nanotopography might influence the biologic activities at the implant–tissue interface.[17] But a great number of TiO_2 particles remained on such fluoride-modified titanium surfaces,[6,17,18] which may have a negative effect on the long-term stability of dental implants.

The loosening of particles during or after implantation endangers the safe application of very rough coatings.[19] Exposure of macrophagelike cells to titanium particles does not affect bone resorption, but inhibits bone formation.[20] The formation of titanium wear particles during the lifetime of an implant is believed to be a major component of loosening because of debris-induced changes in bone cell function. Titanium particles had adverse effects on osteoblast function, resulting in decreased bone formation and integration, but different mechanisms were elicited by particles of different sizes.[21] Phagocytable Ti particles can also induce fibroblastic differentiation.[22] It was demonstrated that small Ti granules that detached from the implant surface were visible at the implant-bone interface of the titanium plasma-sprayed (TPS) implants both at zero time and 14 days after implantation. No material detachment was seen to occur in smooth titanium and SLA implant insertion.[23] A new fluoride-modified microporous titanium surface, which was prepared by sandblasting and dual acid-etching, may decrease or put an end to Ti granules detached from the implant surface into near bone in implant insertion. However, little is known about exactly how osteoblasts respond to this new nanostructural titanium surface.

The present study was designed to investigate the effects of the new nanostructural titanium surface on the morphology, adhesion, and proliferation of MC3T3-E1 osteoblastlike cells, and to evaluate the cell differentiation by measuring the expressions of osteogenic genes and the relevant transcription factors.

MATERIALS AND METHODS

Titanium disk preparation and surface characterization

Pure titanium disks (10.0 × 10.0 × 1.5 mm and 25-mm diameter × 1.5-mm thickness) were machined (Zhejiang Guangci Medical Appliance co. Ltd., Ningbo, China) and treated by large corundum grit blasting, and then etching with a 5.80-mol/L HCl and 8.96-mol/L H_2SO_4 solution. One-half of the disks were subsequently treated in a diluted 0.11 mol/L HF and 0.09 mol/L HNO_3 solution for 10 minutes at room temperature, as the test group; the others were the control group.

Surface topography of titanium disks was determined by Field Scanning Electron Microscopy (FSEM, FEI, SIRION; Hillsboro, OR, USA). X-ray diffraction (XRD; Amsterdam, The Netherlands) patterns of both groups were recorded with an x-ray diffractometer (XRD-98). Superficial surface chemistry of disks was analyzed by x-ray photoelectron spectroscopy (XPS, Kratos AXIS ULTRA DLD; Manchester, England) with monochromatic Al Ka x-rays (8 mA, 15 kV). Surface roughness was tested by portable surface roughness (TR240, Shidai co. Ltd., Beijing, China). Parameters (R_a, R_q, R_{zDIN}, R_t, S_k) were calculated with the affiliated software. Static contact angle was calculated following the sessile drop method using a video-based contact angle system (SL200B, Solon Tech. Inc. Ltd., Shanghai, China) and using ultra pure water as the wetting agent at room temperature. The contact angle measurements were performed at 3 different places of each disk using 3 disks from each group.

Before cell culture, all the disks were ultrasonically cleaned in acetone, 100% alcohol, and distilled water for 15 minutes each, and sterilized with ultraviolet light for 1 hour.

Cell culture and seeding

Mouse preosteoblast cells (MC3T3-E1, Cellbank of Chinese Science Academy, Shanghai, China) were cultured in alpha-Minimum Essential Medium (Gibco, USA) supplemented with 10% fetal bovine serum (Gibco, USA). After confluence, the cells were seeded at a density of 1×10^5 and 1×10^4 cells/well into 6-well and 24-well culture plates (Corning, USA), respectively, to which the disks had been added.

For short-time observation and molecular biology analysis, the disks were prepared directly. For long-time observation and molecular biology analysis, the disks were transferred to new multiwell plates after 1 day of culture so that the cells adhering to cell culture plates instead of disks could be minimized. The cells were then cultured for 2 weeks at 37°C in a humidified 5% CO_2/95% air atmosphere with medium, and the culture medium was replaced every 3 days.

Initial cell attachment and cell proliferation

The disks cultured with cells were treated as described previously.[24] In brief, disks were fixed with 4% paraformaldehyde in 0.1 M phosphate-buffered saline (PBS), PH 7.4, at 4°C for 30 minutes, and were permeabilized with 0.2% Triton X-100 (Sigma, St. Louis, MO) in PBS (Shanghai Sangon Biological Engineering Technology & Services Co, Shanghai, China) to remove the nuclear envelope and soluble nuclear material, and then blocked with 0.5% bovine serum albumin in PBS. Actin microfilaments were identified by 5 μg/mL FITC-labeled phalloidin (Sigma, USA) (green fluorescence); nuclei were stained by 50 μg/mL propidium iodide (Sigma, USA) (red fluorescence). Fluo-

rescence images were photographed using a Nikon Eclipse 80i fluorescence microscope (Nikon Corp., Melville, NY) with DXM1200F CCD.

In the cell morphology study a shape factor was used as described previously.[24,25] The shape factor Ø was expressed as $Ø = 4\pi A/P^2$, where A is the footprint area and P is the perimeter of the cell. The "footprint" of a cell on a porous disk was represented by the biggest outline of the cell projected. A smaller value shape factor indicated greater projection of a cell, which meant better cell spreading. Circular cells have the greatest area-to-perimeter ratio ($Ø = 1$), which means poor cell spreading. The footprint area and perimeter of individual cells were quantified using Image J software (National Institutes of Health, Bethesda, MD, USA). The shape factor was calculated from 30 randomly selected cells on the test and control disks.

For the evaluation of cell attachment and proliferation, cells were cultured on disks in 24-well culture plates for 1, 3, and 6 hours, and 4, 7, and 14 days, and samples were taken for DNA analysis. The DNA content of each cell is generally constant.[9] The cells that attached or proliferated on disk surfaces were determined by the measurement of total DNA content with a PicoGreen dsDNA Quantitation Kit (Invitrogen, USA). At each time point, after medium removal, disks were washed with PBS and covered by 200 μL Na Citrate buffer solution containing 50 mM Na Citrate and 100 mM NaCl, and stored at −80°C until assay. After thawing at room temperature, the cells were scraped and sonicated. Cell lysate (400 μL/well) was aliquoted in triplicate (100 μL) into a 96-well flat-bottomed plate. A 100-μL volume of cell lysate was mixed with 100 μL DNA binding fluorescent dye solution. A fluorescence spectrometer (Sepctra M2, Molecular, USA) was used to read the fluorescent intensity of the mixed solution at an excitation wavelength of 480 nm and emission wavelength of 520 nm against a standard curve.

Alkaline phosphatase activity

Alkaline phosphatase (ALP) activity was measured with a commercial phosphatase substrate kit (Wako, Japan). Following gentle removal of culture medium and washing with PBS, the cells cultured on specimens in 6-well culture plates were lysed by incubation in ALP lysis buffer (CelLytic M, Sigma, USA). The cell lysate was centrifuged for 15 minutes at 4°C and aliquots of supernatants were subjected to total protein assay and to ALP activity measurement. A 20-μL volume of cell lysate was mixed with 100 μL working assay solution, shaken for 1 minute with a plate mixer, and incubated at 37°C for 15 minutes. With the addition of 80 μL of stop solution to each well (96-well culture plate), the reaction was terminated. After that, the mixtures were shaken for another 1 minute and the resulting optical densities were measured at 405 nm with a spectrophotometer (Sunrise-Basic TECAN, Austria). Protein was determined with a BCA protein assay kit (Beyotime, China). Briefly, 20 μL of cell lysate was mixed with 200 μL of working solution and incubated for 30 minutes at 60°C. The resulting optical densities were measured at 562 nm with a spectrophotometer (Sunrise-Basic TECAN). Bovine serum albumin was used to generate a standard curve. ALP activity was expressed as nanomoles of p-nitrophenol liberated per μg of total cellular protein.

Osteocalcin production assay

The production of osteocalcin (OC) by differentiating cells was measured as the release of the ECM protein in the culture medium using Mouse Osteocalcin EIA Kit (Biomedical Technologies, USA). Briefly, 25 μL of cell culture medium sample and 100 μL of osteocalcin antiserum were placed in a 96-well EIA plate and incubated at 4°C for 18 to 24 hours. The well was washed with wash buffer and 100 μL of Streptavidin-horseradish reagent was added, and incubated at room temperature for 30 minutes; 50 μL of TMB solution and hydrogen peroxide solution were then added and incubated at room temperature for 15 minutes. After adding 100 μL of stop solution, absorbance was measured at 450 nm on a spectrophotometer (Sunrise-Basic TECAN). Data are expressed as total ng mouse osteocalcin in the medium per microgram of total cellular protein.

Total RNA extraction, cDNA synthesis and quantitative real-time RT-PCR analysis

Total RNA was isolated from osteoblasts with an RNA isolation kit (Qiagen, Germany). The amount and purity of the RNA samples were measured by optical densitometry at 260 and 280 nm. RNA was converted into complementary DNA (cDNA) using a reverse-transcriptase polymerase chain reaction (RT-PCR) kit (Takara, Japan). Quantitative real-time RT-PCR was performed by Thermal Cycler Dice (Takara TP800, Japan). The sequences of primers for alkaline phosphatase, osteocalcin, type I collagen (Colla I) and β-actin genes are given in Table I. Amplification reactions were performed with a SYBR PrimeScript RT-PCR kit (Takara). A volume of 10 μL of SYBR Premix EX Taq was added to each well of an optical 96-well plate, 0.4 μL of both forward and reverse primer were added, as well as 7.8 μL dH_2O and 2 μL cDNA sample. The plate was covered and centrifuged to remove air bubbles, following PCR quantification using cycling parameters: 95°C, 10 seconds followed by 60°C, 34 sec-

Table I. Forward (F) and Reverse (R) primers for target genes

Gene name	*Amplicon length (bp)*	*5′-3′ primer sequence*
OC	178	F 5′-AGCAGCTTGGCCCAGACCTA-3′
		R 5′-TAGCGCCGGAGTCTGTTCACTAC-3′
ALP	164	F 5′-TGCCTACTTGTGTGGCGTGAA-3′
		R 5′-TCACCCGAGTGGTAGTCACAATG-3′
Colla I	153	F 5′-ATGCCGCGACCTCAAGATG-3′
		R 5′-TGAGGCACAGACGGCTGAGTA-3′
β-actin	131	F 5′-TGACAGGATGCAGAAGGAGA-3′
		R 5′-GCTGGAAGGTGGACAGTGAG-3′

bp, base pairs; *OC,* osteocalcin; *ALP,* alkaline phosphatase; *Colla I,* type I collagen.

onds for 40 cycles. All samples were analyzed in triplicate. The comparative Ct-value method was used to calculate the relative quality of ALP, OC, Colla I, and β-actin. Expression of the housekeeping gene β-actin was used as internal control to normalize results.

Statistical analysis

The cell and biological analyses were performed by using 2 separate runs simultaneously; in each run, all specimens were divided in triplicate. The results were expressed as means and SDs and tested for statistical significance with Student 2-tailed *t* test. A *P* value of .05 or less was considered to indicate statistical significance. All statistical tests were carried out using SPSS (version 12.0; SPSS, Chicago, IL).

RESULTS

Surface characteristic

The surface topography of both groups was similar, which was observed by SEM (Fig. 1). The surface topography revealed a level of macro-pits in the dimension of about 10 to 50 μm, each of which embraced an arrangement of smaller, round-shaped micro-pits with diameters of about 0.5 to 3.0 μm. Some remaining blasting particles were found on the control surfaces. Some discrete nanoprotrusions were observed on the test surface.

The survey spectra of both surfaces showed major peaks at Ti 2p, O 1s, and C 1s (Fig. 2). Relative atom concentrations (at.%) and binding energies (BE) of all elements are summarized in Table II. The content of oxygen and carbon was much higher than that of titanium, and there was little nitrogen and sulfate on the control surface. The carbon and nitrogen were measured lower for the test surface compared with the control, and the oxygen was higher for the test surface. High-resolution spectra of F are presented in Fig. 3.

Phase identification of the elements composing the surface was collected by XRD on one disk from both control and test surfaces. Only titanium and titanium hydride were detected. Peaks at 40.9° and 59.2° indicate the presence of a hydride (TiH_{2-x}). The intensity of the peaks of titanium hydride was lower for test surface as compared with the control surface (Fig. 4).

The parameters of surface roughness are shown in Table III. There were some significant differences between the 2 surfaces. The results indicated that the test surface had more submicro and nanostructures than that of control surface. The surface skewness (S_k) showed the test surface had more intense peaks and fewer deep valleys as compared to the control surface.

The contact angle of control surface was measured as 81.9° ± 7.9°. The test surface was found to be significantly more hydrophobic than the control surface (91.6° ± 6.9°, $P = .015$, $n = 9$).

Fluorescence microscopy

The cellular actin cytoskeleton and cell nucleus after fluorescent staining were evidently shown on both disks (Fig. 5). At 1 hour after cell seeding, cells on both surfaces were alike round, but the pseudopodia were fewer and shorter on control surfaces as compared to test surfaces. Because cells were poorly spread, the actin fibers lapped over nuclei and the color of cells appeared orange. At 3 hours after cell seeding, cells on both surfaces were irregular triangles or polygons, and abundant pseudopodia and actin filaments were observed. The green fluorescence was dark green on cell marginal areas and actin filaments were lacked fidelity because many actin fibers overlapped. After 1 day and 3 days of cell culturing, cells on both surfaces were irregular triangles or fusiforms, actin filaments were reticular and spread full cytoplasm, and long strip pseudopodia were observed.

The shape factor values changed correspondingly to the change in cell morphology (Table IV). At 1 hour and 24 hours after cell seeding, the mean Ø value of cells on test disks was similar with that on control disks. At 3 hours and 3 days after cell seeding, the mean Ø value of cells on test disks was significantly smaller than on control disks.

DNA content

The cells' attachment and adhesion happened minutes to hours after cell seeding, and cell migration, proliferation, and differentiation happened days to weeks after cell seeding,[22] so the DNA content at different cell culture periods could correspondingly indicate cell attachment, adhesion, and proliferation. The mean DNA content at 1 hour, 3 hours, 6 hours, and 4 days, 7 days, and 14 days after MC3T3-E1 cell seeding is shown in Fig. 6. The mean DNA content gradually decreased from 1 hour to 6 hours after cell seeding, and

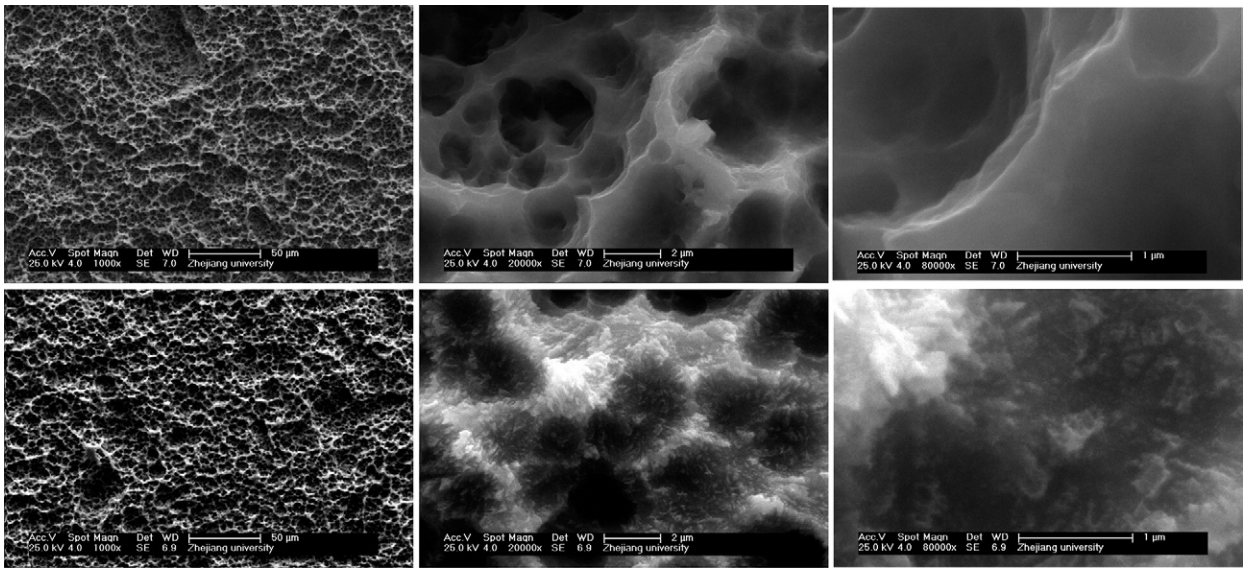

Fig. 1. Scanning electron microscopic evaluation of 2 group disks. The upper images show the control group and the lower imagers show the test group.

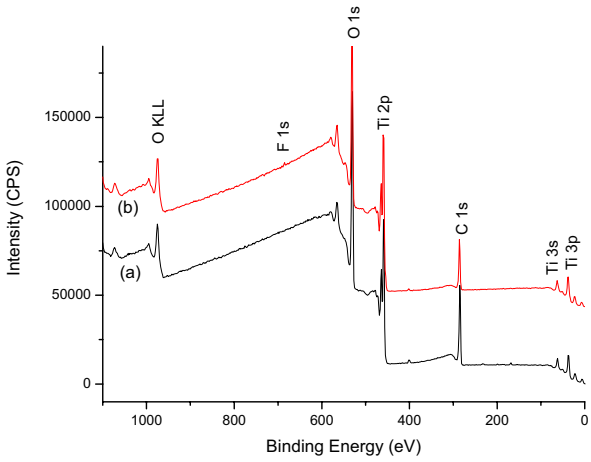

Fig. 2. Survey XPS spectra. (**a**) XPS spectra of the control surface; (**b**) XPS spectra of the test surface.

evidently increased from 6 hours to 14 days on both groups. At 1 hour and 3 hours, the mean DNA content on control surfaces was more than that on test surfaces. At 14 days, the mean DNA content on test surfaces was more than that on control surfaces.

Alkaline phosphatase activity and osteocalcin production assay

After 4 and 7 days of culture, the alkaline phosphatase activity was evidently higher on the test surface than on the control surface. But after 14 days of culture, the alkaline phosphatase activity was higher on the control surface than on the test surface (Fig. 7). After 14 days of culture, there was no significant difference in the osteocalcin secreted by cells.

Quantitative real-time RT-PCR analysis

The relative expression of alkaline phosphatase mRNA at 4 days after cells were cultured on the control surface was used as the reference value, which was uniform by the internal standard gene (β-actin) and the magnitude of deviation of gene relative expression was calculated by $2^{-\Delta\Delta CT}$. The relative expression of Colla I, ALP, and OC mRNA by MC3T3-E1 cells after 4, 7, and 14 days of culture on both group surfaces are shown in Fig 8. The relative expression of OC and ALP mRNA was low at 4 and 7 days after cell culture, and significantly increased at 14 days. After 4 days of culture, the relative expression of Colla I and OC mRNA on the test surface was significantly higher than that on the control surface. But after 7 days of culture, the relative expression of OC and ALP mRNA on the control surface was significantly higher than that on the test surface. After 14 days of culture, the relative expression of ALP mRNA on the control surface was also significantly higher than that on the test surface.

DISCUSSION

To enhance osseointegration, dental implant surfaces should possess the ability to stimulate differentiation of osteogenic cells and matrix formation. Surface chemistry, surface morphology, and roughness influence cell-biomaterial interactions and bone formation on ti-

Table II. Binding energies and atom concentration rate (at.%) of elements at as-received and sputter-cleaned implants in XPS analysis

	C		O		Ti		F		N		S	
Surface	*at.%*	*BE*	*at.%*	*BE*	*at.%*	*BE*	*at.%*	*BE*	*at.%*	*BE*	*at.%*	*BE*
control	44.6	285.3	39.1	530.8	14.5	459.3	—	—	1.1	400.5	0.7	169.4
test	33.9	285.4	45.5	530.7	19.0	459.3	0.8	684.4	0.8	400.3	—	—

XPS, X-ray photoelectron spectroscopy; BE, binding energy.

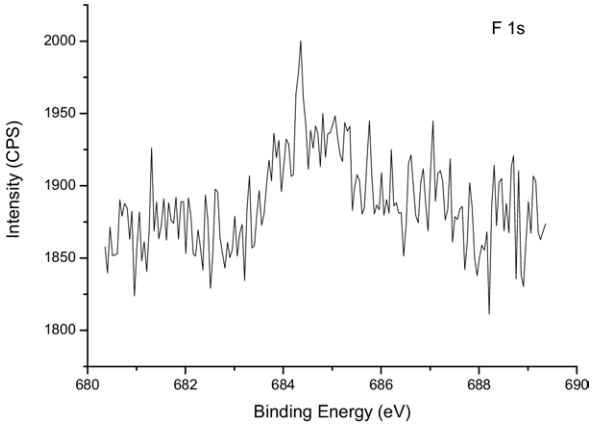

Fig. 3. High-resolution XPS spectra of the test surface: F 1s spectra.

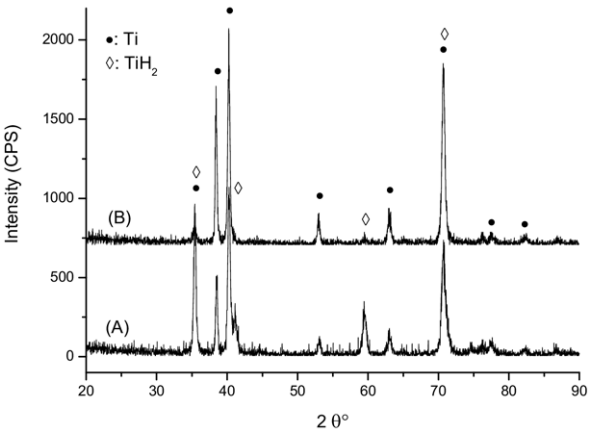

Fig. 4. XRD patterns: (**A**) control surface; (**B**) test surface.

tanium implants of various designs and surface preparations.[26] The initial attachment and subsequent cell behavior included 5 steps: (1) deposition of serum factors on substratum (seconds), (2) cellular attachment (minutes), (3) spread and formation of focal contact/cellular adhesion (hours), (4) polarization, and (5) migration and secretion of cytokines and extracelluar matrix or colony formation (days to weeks).[22,27] Some studies supported the hypothesis that surface roughness may have direct effects on osteoblast migration, attachment, proliferation, and differentiation.[28] Studies showed that cells cultured on Ti surfaces with microrough features exhibit reduced proliferation and enhanced differentiation when compared with cells grown on tissue culture plastic or smooth Ti substrates.[29,30] It was reported that 100-μm cavities favored osteoblast attachment and growth, the submicro-scale etch enhanced differentiation and TGF-β1 production.[31] But it also reported that there are no differences in cell proliferation and differentiation on surfaces treated by blasting and etching.[28]

From cell morphological observation, the cells on the test surface had more pseudopodia than those on the control surface. Especially after 3 hours and 3 days of culture, the cell shape factor of the test surface was obviously smaller than that of the control surface, osteoblasts on the test surface showed more clear stress fiber and tiny pseudopodia spreading all round. This result indicated that osteoblasts had accomplished spreading and cellular adhesion after 3 hours of cell seeding, and also showed cell adhesion on the test surface tightly and suggested the surface was in favor of cells spreading and adhesion at early stage. The results were similar to our previous study[24] and other reports.[32] The quantity of focal adhesion plaque on fluoride ion–implanted titanium was more than that on the nonimplanted titanium after 6-hour MG-63 cell culture,[32] and the full range XPS spectra indicated that the surface of fluoride ion–implanted titanium was the mixture of titanium dioxide and titanium trifluoride. The shape factor value became larger after 1 and 3 days of culture; this may be because the adhesion cells started proliferating and migrating, and then spreading and adhesion again. However, the shape factor can only reflect the cell morphology that attached onto the surface and cannot reflect the cell number on the surface of titanium disks.

The DNA content of each cell is metastable; for example, the DNA content in 10^6 mouse cells is about 5.8 μg.[9] For this reason, measuring the DNA content of cells on the surface at different experimental periods can presume the cell number on disks, which can indirectly reflect the information of cell attachment and pro-

Table III. Surface roughness, mean values with standard error are presented (n = 6)

Surface	R_a (μm)	R_q (μm)	R_{zDIN} (μm)	R_t (μm)	S_k (μm)
Test	1.91 ± 0.38	2.29 ± 0.39	9.12 ± 0.67	10.14 ± 0.05	0.05 ± 0.22
Control	1.26 ± 0.45	1.59 ± 0.49	7.37 ± 1.16	9.42 ± 0.92	−0.37 ± 0.65
P	.022	.023	.012	.117	.168

R_a, the arithmetic average of the absolute height values of all points of the profile; R_q, the root mean square of the value of all points of the profile; R_{zDIN}, The arithmetic average of the maximum peak to valley height of the roughness values z(x1) to z(x5) of 5 consective sampling sections over the filtered profile; R_t, the maximum peak-to-valley height of the entire measurement trace; S_k, amplitude distribution skew; $S_k<0$, profile with "plateaus" and single deep valleys; $S_k>0$, profile with very intense peaks.

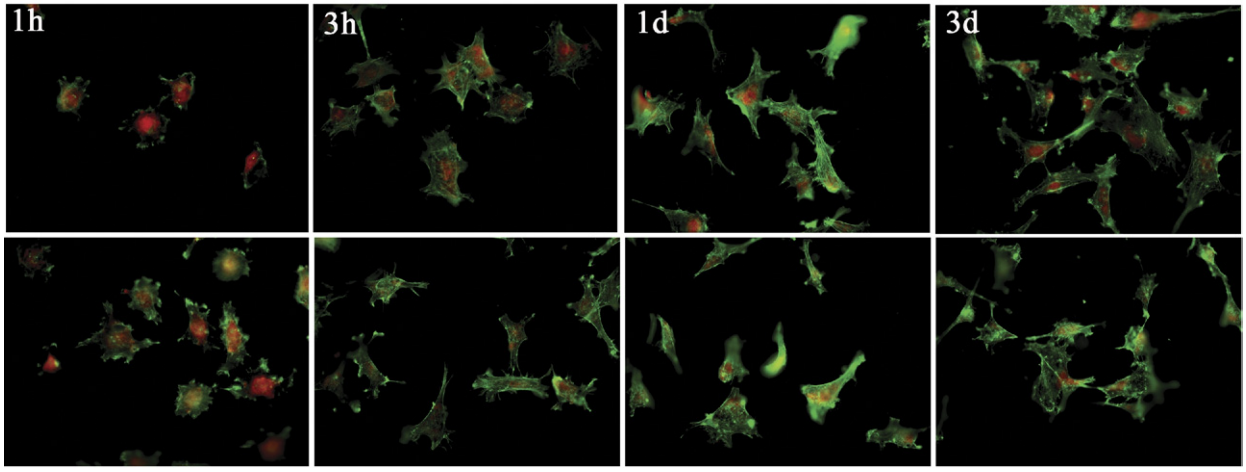

Fig. 5. Fluorescence microscopic images show cellular actin cytoskeleton and cell nucleus on the test surfaces (*lower*) and control surfaces (*upper*).

Table IV. The shape factor (Ø) of cells on different surfaces (mean ± SD, n = 30)

Surface	*1 h*	*3 h*	*24 h*	*3 d*
Control	0.42 ± 0.12	0.31 ± 0.11	0.30 ± 0.09	0.34 ± 0.12
Test	0.43 ± 0.14	0.25 ± 0.08*	0.32 ± 0.09	0.28 ± 0.09†

*P = .046.
†P = .032.

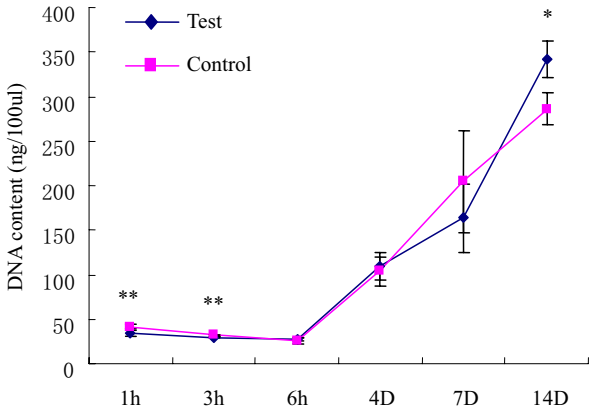

Fig. 6. The mean DNA content on both groups, which reflects the number of MC3T3-E1 cells attached and proliferated on 2 type surfaces (n = 6, *P < .05, **P < .01).

liferation. The DNA content on the control surface was evidently higher than that on test surface at 1 and 3 hours after cell seeding. The DNA content was similar to both surfaces at 6 hours, 4 days, and 7 days and significantly higher on the test surface at 14 days. These results were not consistent with Lamolle et al.'s investigation,[9] who demonstrated that the disks containing a relatively high concentration of fluoride were significantly less cytotoxic and possessed a higher number of attached cells than the control disks after 7 days of culture.

Colla I is an early marker expressed during the proliferation stage of osteoblastic cells, followed by ALP in the matrix maturation stage, and OC related to calcium deposition in the extracellular matrix under its mineralization period.[33] In this study, the Colla I relative mRNA levels were higher for the test surface compared with the control surface after 4 days of cul-

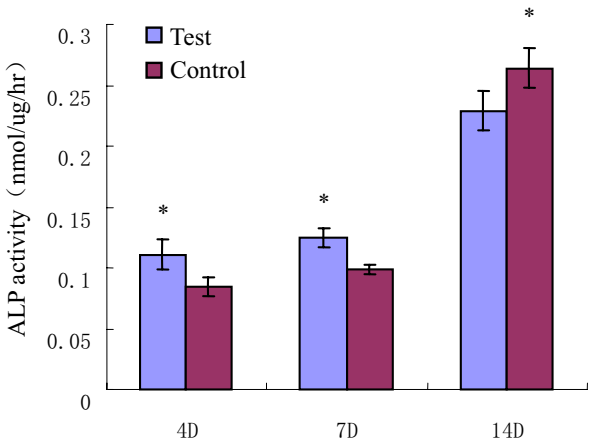

Fig. 7. Alkaline phosphatase activity of MC3T3-E1 cells after 4, 7, and 14 days of culture on both surfaces (n = 6, $*P < .05$).

ture. But after 7 and 14 days of culture, although Colla I relative mRNA levels were higher for the test surface compared with the control, no significant difference was found. So the results were similar to Lamolle et al.'s; namely, the Colla I relative mRNA levels were higher for all the HF modified surfaces compared with the control. But no significant difference was found after 7 days of culture.[9] The results of DNA content and Colla I mRNA expression indicated that HF/HNO_3-modified surface cannot enhance cell attachment during early stages after cell seeding, but this surface can enhance attached cell proliferation.

This study also showed that HF/HNO_3-modified surface can promote MC3T3-E1 cell synthesis ALP at an early stage, and showed that OC gene expression was significantly increased on this new surface as compared with the control surface at 4 days after cell seeding. But at 7 days after cell seeding, ALP and OC gene expression was significantly increased on the control surface as compared with the test surface. This indicated that an HF/HNO_3-modified surface could enhance cell differentiation during early stages, but the cell differentiation on the control surface could catch up with and even exceed an HF/HNO_3-modified surface at a later stage. These results had slight differences with other reports. Fluoride modification of titanium surfaces has been shown to enhance both proliferation and differentiation of mesenchymal stem cells and pre-osteoblasts.[7-9,34,35] At 24 hours, cells adherent to fluoride treatment surface displayed greater proliferation than the surfaces that did not receive fluoride treatment, and a trend of low proliferation with increasing fluoride treatment was noted at 24 hours and may reflect earlier commitment to differentiation.[7] RUNX-2 and Osterix levels were significantly increased on the TiO_2/HF surfaces as compared with the TiO_2 and smooth surfaces through the MC3T3-E1 cell cultural period.[8] It was also reported that although Colla I-relative mRNA levels were higher for all the HF-modified surfaces compared with the control, no significant difference was found after 7 days of culture; ALP and OC relative mRNA levels showed no difference between control and tested surfaces after 7 days.[9] It was found that Cbfa1/RUNX-2 gene expression was significantly increased on Osseospeed and TiOBlast surface as compared with grit-blasted and etched (SLA-1) and grit-blasted, etched, and rinsed with N_2 protection and stored in isotonic NaCl (SLA-2)

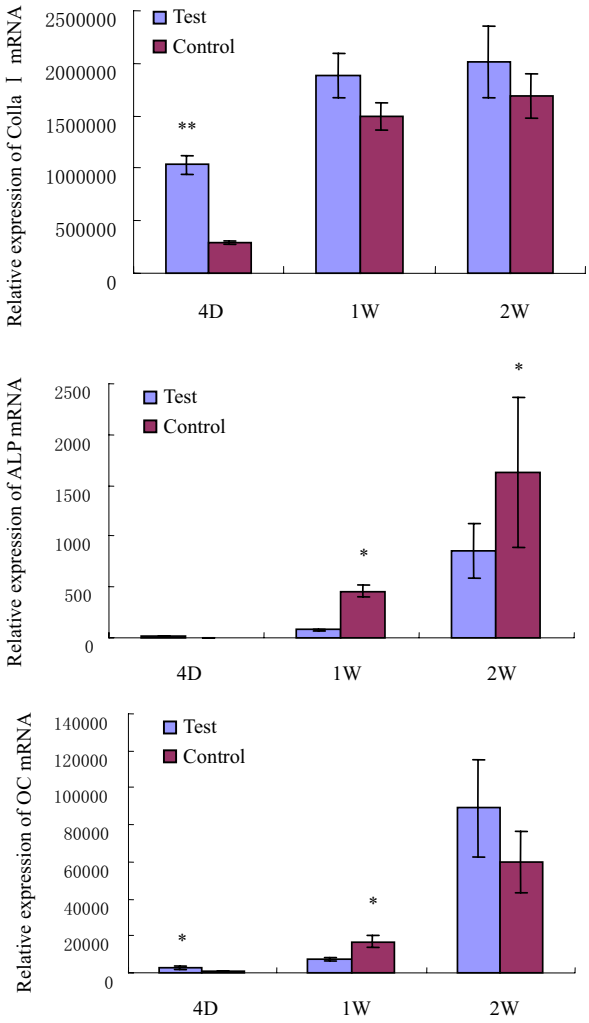

Fig. 8. Relative expression of Colla I, ALP, and OC mRNA of MC3T3-E1 cells after 4, 7, and 14 days of culture on both surfaces in the presence of basic medium. Relative mRNA abundance was determined by the $2^{-\Delta\Delta CT}$ method and reported as relative quality. β-actin was used for normalization (n = 6, $*P < .05$; $**P < .01$).

surfaces. And there was no significant difference among titanium discs in osteocalcin and bone sialoprotein (BSPII) gene expression.[34] But Isa et al.[6] reported that the different surfaces did not alter the mRNA expression for ALP, Colla I, osterix, osteocalcin, or BSP II. Inconsistent results were reported, which may have been caused by the different cells, surface treatments, and surface roughness.

CONCLUSION

The surface treatment with HF/HNO_3 solution produces a nanostructural porous surface with fluoride, hydrogen ions. This new surface could commit MC3T3-E1 cell proliferation and differentiation at an early stage. These results suggested that the nanostructural surface and fluoride, hydrogen ions might promote the attachment, proliferation, and differentiation of preosteoblasts.

REFERENCES

1. Giordano C, Sandrini E, Busini V, Chiesa R, Fumagalli G, Giavaresi G, et al. A new chemical etching process to improve endosseous implant osseointegration: in vitro evaluation on human osteoblast-like cells. Int J Artif Organs 2006;29:772-80.
2. Albrektsson T, Wennerberg A. Oral implant surfaces: Part 1—review focusing on topographic and chemical properties of different surfaces and in vivo responses to them. Int J Prosthodont 2004;17:536-43.
3. Buser D, Schenk RK, Steinemann S, Fiorellini JP, Fox CH, Stich H. Influence of surface characteristics on bone integration of titanium implants. A histomorphometric study in miniature pigs. J Biomed Mater Res 1991;25:889-902.
4. Klokkevold PR, Nishimura RD, Adachi M, Caputo A. Osseointegration enhanced by chemical etching of the titanium surface. A torque removal study in the rabbit. Clin Oral Implants Res 1997;8:442-7.
5. Buser D, Nydegger T, Oxland T, Cochran DL, Schenk RK, Hirt HP, et al. Interface shear strength of titanium implants with a sandblasted and acid-etched surface: a biomechanical study in the maxilla of miniature pigs. J Biomed Mater Res 1999;45:75-83.
6. Isa ZM, Schneider GB, Zaharias R, Seabold D, Stanford CM. Effects of fluoride-modified titanium surfaces on osteoblast proliferation and gene expression. Int J Oral Maxillofac Implants 2006;21:203-11.
7. Cooper LF, Zhou Y, Takebe J, Guo J, Abron A, Holmen A, et al. Fluoride modification effects on osteoblast behavior and bone formation at TiO2 grit-blasted c.p. titanium endosseous implants. Biomaterials 2006;27:926-36.
8. Guo J, Padilla RJ, Ambrose W, De Kok IJ, Cooper LF. The effect of hydrofluoric acid treatment of TiO2 grit blasted titanium implants on adherent osteoblast gene expression in vitro and in vivo. Biomaterials 2007;28:5418-25.
9. Lamolle SF, Monjo M, Rubert M, Haugen HJ, Lyngstadaas SP, Ellingsen JE. The effect of hydrofluoric acid treatment of titanium surface on nanostructural and chemical changes and the growth of MC3T3-E1 cells. Biomaterials 2009;30:736-42.
10. Ellingsen JE. Pre-treatment of titanium implants with fluoride improves their retention in bone. J Mater Sci Mater Med 1995:749-53.
11. Ellingsen JE, Johansson CB, Wennerberg A, Holmen A. Improved retention and bone-to-implant contact with fluoride-modified titanium implants. Int J Oral Maxillofac Implants 2004;19:659-66.
12. Berglundh T, Abrahamsson I, Albouy JP, Lindhe J. Bone healing at implants with a fluoride-modified surface: an experimental study in dogs. Clin Oral Implants Res 2007;18:147-52.
13. Abrahamsson I AJ-P, Berglundh T. Healing at fluoride-modified implants placed in wide marginal defects: an experimental study in dogs. Clin Oral Implants Res 2008;19:153-9.
14. Stanford CM, Johnson GK, Fakhry A, Gratton D, Mellonig JT, Wanger W. Outcomes of a fluoride modified implant one year after loading in the posterior-maxilla when placed with the osteotome surgical technique. Appl Osseointegration Res 2006;5:50-5.
15. Ellingsen JE, Thomsen P, Lyngstadaas SP. Advances in dental implant materials and tissue regeneration. Periodontol 2000 2006;41:136-56.
16. Mendonca G, Mendonca DB, Aragao FJ, Cooper LF. Advancing dental implant surface technology—from micron- to nanotopography. Biomaterials 2008;29:3822-35.
17. Fandridis J, Papadopoulos T. Surface characterization of three titanium dental implants. Implant Dent 2008;17:91-9.
18. Kang BS, Sul YT, Oh SJ, Lee HJ, Albrektsson T. XPS, AES and SEM analysis of recent dental implants. Acta Biomater 2009;5:2222-9.
19. Vercaigne S, Wolke JG, Naert I, Jansen JA. Histomorphometrical and mechanical evaluation of titanium plasma-spray-coated implants placed in the cortical bone of goats. J Biomed Mater Re. 1998;41:41-8.
20. Tsutsui T, Kawaguchi H, Fujino A, Sakai A, Kaji H, Nakamura T. Exposure of macrophage-like cells to titanium particles does not affect bone resorption, but inhibits bone formation. J Orthop Sci 1999;4:32-8.
21. Choi MG, Koh HS, Kluess D, O'Connor D, Mathur A, Truskey GA, et al. Effects of titanium particle size on osteoblast functions in vitro and in vivo. Proc Natl Acad Sci U S A 2005;102:4578-83.
22. Jager M, Zilkens C, Zanger K, Krauspe R. Significance of nano- and microtopography for cell-surface interactions in orthopaedic implants. J Biomed Biotechnol 2007;2007:69036.
23. Franchi M, Bacchelli B, Martini D, Pasquale VD, Orsini E, Ottani V, et al. Early detachment of titanium particles from various different surfaces of endosseous dental implants. Biomaterials 2004;25:2239-46.
24. Yang XF, Chen Y, Yang F, He FM, Zhao SF. Enhanced initial adhesion of osteoblast-like cells on an anatase-structured titania surface formed by H2O2/HCl solution and heat treatment. Dent Mater 2009;25:473-80.
25. Schuler M, Owen GR, Hamilton DW, de Wild M, Textor M, Brunette DM, et al. Biomimetic modification of titanium dental implant model surfaces using the RGDSP-peptide sequence: a cell morphology study. Biomaterials 2006;27:4003-15.
26. Bagno A, Di Bello C. Surface treatments and roughness properties of Ti-based biomaterials. J Mater Sci Mater Med 2004;15:935-49.
27. Goto T, Yoshinari M, Kobayashi S, Tanaka T. The initial attachment and subsequent behavior of osteoblastic cells and oral epithelial cells on titanium. Biomed Mater Eng 2004;14:537-44.
28. Bachle M, Kohal RJ. A systematic review of the influence of different titanium surfaces on proliferation, differentiation and protein synthesis of osteoblast-like MG63 cells. Clin Oral Implants Res 2004;15:683-92.

29. Schwartz Z, Lohmann CH, Oefinger J, Bonewald LF, Dean DD, Boyan BD. Implant surface characteristics modulate differentiation behavior of cells in the osteoblastic lineage. Adv Dent Res 1999;13:38-48.
30. Kim MJ, Kim CW, Lim YJ, Heo SJ. Microrough titanium surface affects biologic response in MG63 osteoblast-like cells. J Biomed Mater Res A 2006;79:1023-32.
31. Zinger O, Zhao G, Schwartz Z, Simpson J, Wieland M, Landolt D, et al. Differential regulation of osteoblasts by substrate microstructural features. Biomaterials 2005;26:1837-47.
32. Liu HY, Wang XJ, Yi Z, Wang LP, Wang XF, Ai HJ. [Influence of fluoride ion-implanted titanium on the formation of focal adhesion plaque in vitro]. Hua Xi Kou Qiang Yi Xue Za Zhi 2008;26:137-139, 143. Chinese.
33. Stein GS, Lian JB, Stein JL, Van Wijnen AJ, Montecino M. Transcriptional control of osteoblast growth and differentiation. Physiol Rev 1996;76:593-629.
34. Masaki C, Schneider GB, Zaharias R, Seabold D, Stanford C. Effects of implant surface microtopography on osteoblast gene expression. Clin Oral Implants Res 2005;16:650-6.
35. Monjo M, Lamolle SF, Lyngstadaas SP, Ronold HJ, Ellingsen JE. In vivo expression of osteogenic markers and bone mineral density at the surface of fluoride-modified titanium implants. Biomaterials 2008;29:3771-80.

Reprint requests:

Shifang Zhao, MD, DDS
Department of Oral and Maxillofacial Surgery
The Affiliated Stomatology Hospital
School of Medicine
Zhejiang University
Yan'an Road 395#
Hangzhou, Zhejiang Province, China
shifangzhao@yahoo.com.cn